ISBN: 978-3-95450-225-7 ISSN: 2673-5571 doi:10.18429/JACoW-HB2021-WEDC2

ACCELERATION OF THE HIGH CURRENT DEUTERON BEAM THROUGH THE IFMIF-EVEDA RFQ: CONFIRMATION OF THE DESIGN BEAM DYNAMICS PERFORMANCES

L. Bellan†, L. Antoniazzi, M. Comunian, E. Fagotti, F. Grespan, M. Montis, , M. Giacchini, A. Palmieri, M. Poggi, F. Scantamburlo, A. Pisent INFN-LNL, Legnaro, Italy
B. Bolzon, N. Chauvin, J. Marroncle, CEA-IRFU, Gif-sur-Yvette, France
T. Akagi, K. Masuda, K. Kondo, M. Sugimoto, QST, Aomori, Japan
P. Cara, IFMIF/EVEDA Project Team, Aomori, Japan
D. Jimenez-Rey, I.Podadera, CIEMAT, Madrid, Spain
I. Moya, H. Dzitko, C. Yann, F4E, Garching, Germany

Abstract

The Linear IFMIF Prototype Accelerator (LIPAc) is a high intensity D^+ linear accelerator; demonstrator of the International Fusion Material Irradiation Facility (IFMIF). In summer 2019 the IFMIF/EVEDA Radio Frequency Quadrupole (RFQ) accelerated its nominal 125 mA deuteron (D+) beam current up to 5 MeV, with >90% transmission for pulses of 1 ms at 1 Hz, reaching its nominal beam dynamics goal. The paper presents the benchmark simulations and measurements performed to characterize the as-built RFQ performances, in the low and high perveance regime. In this framework, the commissioning strategy with a particular focus on the reciprocal effects of the low-medium energy transfers lines and the RFQ is also discussed. In the last part of the paper, the future commissioning outlooks are briefly introduced.

INTRODUCTION

The accelerator setup of LIPAc [1] for the pulse commissioning of the RFQ was composed by the ECR high intensity deuteron ion source [2], the Radio-Frequency Quadrupole [3] and the Medium Energy Transfer Line [4] coupled with a diagnostic plate [5]. The line was terminated with a temporary low power beam dump, with a maximum sustainable DC of 0.1%. First D^+ injection was possible in March 2019, then we reached in July 132 kV-2.5 ms-20 Hz and in July 24th we achieved a 125 mA D+ current at 1 ms/1 Hz out the RFQ, with transmission>90%. In order to identify the RFQ performances, it was important to separate the effects on the transmission of the preceding and subsequent parts of the accelerator.

THE RFQ

The Radio Frequency Quadrupole is a 4-vane 9.8 m CW accelerator which accelerates 125 mA positive deuteron beam from 100 keV up to 5 MeV. The maximum Kilpatrick at its nominal file is 1.76. During the RF conditioning at LNL, 1.94 value was reached in the CW regime for 5 hours with the third section of the RFQ. At the state of the art, at the Rokkasho site, in Japan, we reached 1.85 value during pulse conditioning, and we are under high D.C. conditioning of the whole assembly. [6].

† luca.bellan@lnl.infn.it

Some design parameters of the RFQ are shown in Fig. 1. The details are reported in reference [7]. However, it is worth re-calling some features that are relevant for this paper:

- The generalized perveance of the nominal beam, from the low energy up to the high section of the accelerator ranges from 10^{-3} to 10^{-5}.
- The tune depression from the shaper is roughly constant, $\frac{\sigma_t}{\sigma_{0,t}} = 0.5$ and $\frac{\sigma_l}{\sigma_{0,l}} = 0.4$
- The input/output beam normalized rms emittance are 0.25/0.26 mm mrad for the transverse plane while the longitudinal rms emittance is 0.2 MeV deg.

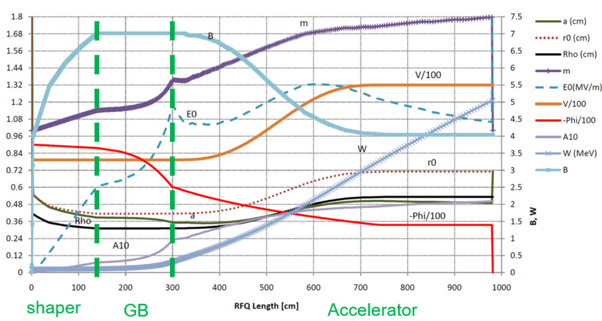

Figure 1: Design parameters of the IFMIF/EVEDA RFQ.

During the Critical Design review, in order to decrease the input beam requirements from the Low Energy Transfer Beam (LEBT) section, easing the beam matching to the RFQ focusing channel, it was decided to decrease the RFQ focusing factor B defined by Eq. (1) smoothly, after the RMS (Radial Matching Section) up to the shaper end, following the undepressed longitudinal phase advance of the RFQ.

$$B = \frac{qV\lambda^2}{mc^2 r_0^2} \quad (1)$$

The net effect is a drop of the input beam convergence requirements. In particular

- the rms value of the X′ decreases from 43 mrad down to 24 mrad.
- the transmission of the accelerated particles drops form the previous design 95% down to 93.7%.

ISBN: 978-3-95450-225-7 ISSN: 2673-5571 doi:10.18429/JACoW-HB2021-WEDC2

The transmission was estimated considering a 4D Gaussian distributed beam, truncated at 4 σ, with an input current of 130 mA, with a 0.25 mm mrad rms normalized transverse emittance. The software used for the RFQ modelling was TOUTATIS [8]: its ability to change the voltage and the vane profile was a key feature for the implementation of the as-built RFQ model. Other parameters of the RFQ can be found in Table 1.

Table 1: Main RFQ Parameters

Input/output Energy	0.1-5	MeV
Duty cycle	cw	
Dueteron beam current	125	mA
Operating Frequency	175	MHz
Length (5.7 λ)	9.78	m
Vg (min-max)	79-132	kV
R0 (min-max) ρ/R0=0.75	0.4135-0.7102	cm
Total Stored Energy	6.63	J
Cavity RF power dissipation	550	kW
Maximum dissipated power	86	kW/m
Power density (average-max)	3.5-60	kW/cm^2
Q_0/Q_{sf}=0.82	13200	
Shunt impedance(<V^2>)L/P_d	201	KΩ-m
Frequency tuning	Water temp.	
N cells (βλ/2)	489	

As-built RFQ

In order to further improve the precision of our simulations with respect the experiments, we implemented the mechanical errors of the RFQ modules and the bead pull measurements after tuning [9]. In this case, the beam transmission further decreases of about 2%, while the transverse and longitudinal emittances increase. Table 2 summarizes the new values of the transmission and emittance increase

Table 2: Mechanical and Bead Pull Errors on Beam Transmissions and Emittances

Parameters	**Values**
$\Delta\varepsilon_{rms,t,n}/\varepsilon_{rms,t,n}$	+3%
$\Delta\varepsilon_{rms,l}/\varepsilon_{rms,l}$	+8%
$\Delta Tr./Tr$	-2% (i.e., 91.8%)

The as-built RFQ was implemented in all the simulations involved during the commissioning and beam characterization.

Criteria for Larger than 90% of Transmission

The beam coming from the high intensity ion source is not in an equilibrium distribution: its phase-space distribution is hardly comparable with a well-known stationary phase space distributions or even to the most common design-used distributions, such as the waterbag, gaussian and KV. It more often shows the characteristics of hollow and halo distribution. In order to decrease the dependence of the RFQ design with respect the particle distribution, we performed the RFQ design following the evolution of the equivalent beam rms quantities (relying on the Sacharer equivalent principle) [3]. We used the same philosophy for evaluating the input beam requirements from the LEBT: for any beam current $I_{b,}$ exists a maximum rms normalized transverse emittance $\varepsilon_{Gaussian,rms,t,n}$ of the equivalent Gaussian beam that allows to transmit > 90%, with rms matched conditions. If the current is negligible the $\varepsilon_{Gaussian,t,n}$ (total emittance) becomes comparable with the well-known geometric acceptance A, in particular $\varepsilon_{Gaussian,t,n} = 4\,\varepsilon_{Gaussian,rms,t,n} = 1.1$

The larger acceptance of the lower current beam results in the possibility to allow a larger mismatch with lower current beam. As an example, for 7 mA proton beam the acceptable mismatch [10] increases up to 220%. These two last considerations where extensively used for the probe beam (low current low emittance beam) first commissioning.

THE INJECTOR

The injector, an the ECR (Electron Cyclotron Resonance) ion source, consists of a 2.45 GHz RF power source with two coils magnetic structure. The nominal CW beam extracted consists of 140 mA D+ at 100 kV. For commissioning purposes, the source can also extract tens of mA of H+ at 50 kV and can work in pulse mode. From the beam dynamics point of view, these beams are characterized by a high perveance beam transport: the general perveance (un-compensated) ranges from 5×10^{-4} for the probe up to 5×10^{-3} nominal beam. In order to preserve the beam quality from the ion source up to the RFQ injection point (the LEBT), two magnetic solenoids and two repellers, one in the extraction and one at the RFQ entrance, are used in order to allow the space-charge compensation to take place.

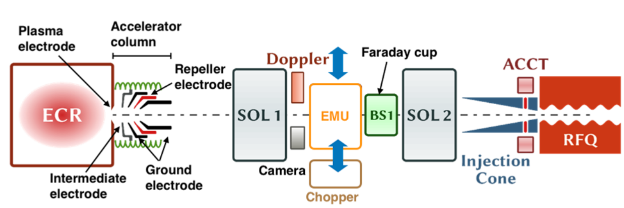

Figure 2: Sketch of the IFMIF/EVEDA injector.

The solenoids need to be tuned in order to match the output beam characteristics from the source exit to the RFQ input, while the steerers (integrated into the solenoids) set to 0 the first order moments of the beam at injection point. A permanent diagnostic box was installed between the two solenoids.

ISBN: 978-3-95450-225-7 ISSN: 2673-5571 doi:10.18429/JACoW-HB2021-WEDC2

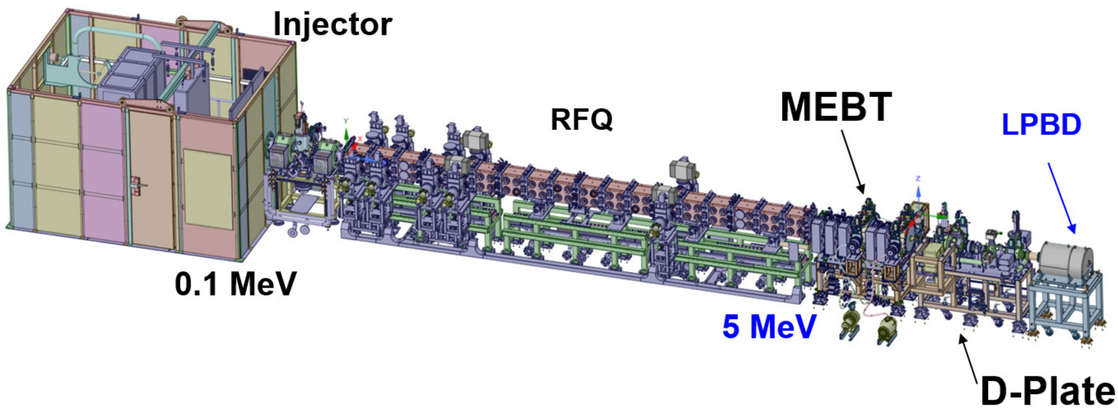

Figure 3: Sketch of the accelerator during RFQ pulsed commissioning.

During the injector commissioning a second diagnostic box in place of the RFQ was used. Figure 2 shows the sketch of the injector in its nominal configuration (see Fig. 3 for the sketch of whole setup).For this configuration the source is equipped with a diagnostic box between the two solenoids which contains an Allison type emittance-meter, the Doppler shift spectrometers and CCD camera. The aim of the ion source, from the RFQ point of view, is to produce a 125 mA D^+ with an $\varepsilon_{rms,t,n} < 0.3$ mm mrad (at RFQ in-jection), the $\varepsilon_{Gaussian,rms,t,n}$ for 125 mA. It is difficult to measure the phase spaces at the RFQ injection point, since the envelopes are small and the power density high. There-fore, the input beam emittance and Twiss must be estimated via the combination of appropriate beam dynamics models [11] and the measurements

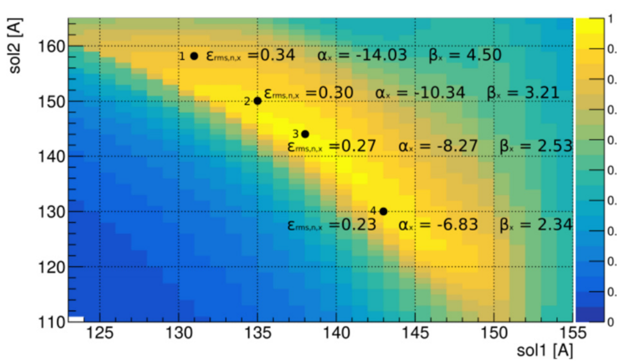

Figure 4: 85 mA proton beam at 50 keV measured transmission plot, during injector commissioning, with a second diagnostic box in place of the RFQ. Superimposed to the plot, the measured emittances are shown, after 300 mm from the injection point.

In particular, the estimation of the emittance growth along the LEBT is very important for the characterization of the emittance at RFQ input. During the injector commissioning we found out that the emittance had a trend with respect the solenoids values of the LEBT. Fig. 4 shows the measured solenoids scan plot of the transmission through the injection cone up to the end of second diagnostic box that was placed in place of the RFQ. Superimposed to that plot the measured emittance values after 300 mm with respect the RFQ injection point are shown. The major reasons of the emittance increase were identified, confirmed by the simulations [15], due to the solenoid aberrations and uncompensated space-charge fields. The beam considered in Fig. 4 is an 85 mA proton beam at 50 keV. The emittance shows the higher values near the matched positions, in the left high part of the plot. Therefore, in order to be sure to not lowering the emittance quality at the RFQ input while changing the solenoids for the matching procedure, we developed a criterion that helps up to evaluate the injector working point without the second diagnostic box:

- we choose a specific value of the first solenoid that correspond to a beam parallel transport between the solenoids.
- we measure the emittance for various injector configurations.

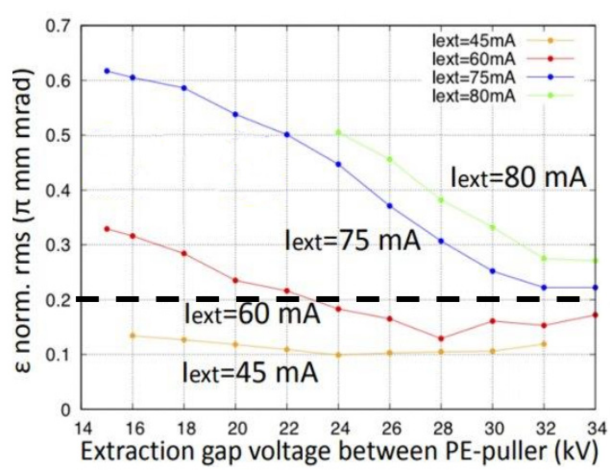

Figure 5: Example of several source tunings: the emittance is measured between the two solenoids with respect the puller voltage. The black dotted line shows the criterion limit for injecting into the RFQ.

If $\varepsilon_{rms,t,n} < 0.2$ mm mrad, then the margin for the emittance growth was considered safe for injecting the beam into the RFQ. Fig. 5 shows an example of the application of such criteria for several proton beam extractions. The software used during the RFQ beam commissioning are,

ISBN: 978-3-95450-225-7 ISSN: 2673-5571 doi:10.18429/JACoW-HB2021-WEDC2

for the extraction, IBSIMU [16], while WARP [17] and Tracewin [18] for the LEBT transport.

THE MEBT

The MEBT (Medium Energy Beam Transfer) line of 2.3 m length, composed by 5 magnetic quadrupoles, for the transverse matching to the SRF, and 2 bunchers, for the longitudinal matching. The beam generalized perveance is, for the nominal beam, 10^{-5}. Fig. 6 shows the sketch of the MEBT. The MEBT is equipped also with two scrapers positioned between the first three quadrupoles, as well as with BPMs for the beam phase and TOF measurements along the line and current monitors.

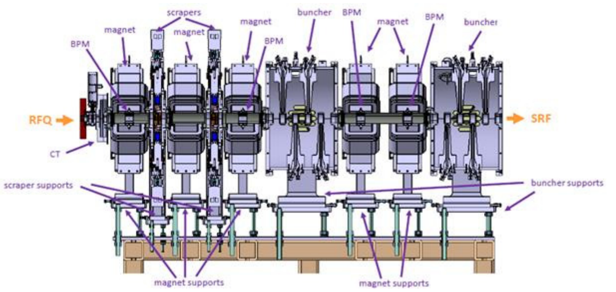

Figure 6: Sketch of the optics element of the MEBT and its diagnostics.

The diagnostic plate was attached after the MEBT. The diagnostic plate implements a system for the emittance measurements through the method of slits and grids. The method was further improved thanks to the usage of a magnetic steerers. The details are presented in reference [19]. Beside the diagnostics, the beam dynamics of the MEBT includes another hindered attribute: it can separate, through the strong chromatism effects, the not accelerated particles (i.e. the particles that are not captured by the separatrix) and the residual contaminants presents at the RFQ injection point that survived within the RFQ channel. (see Fig. 3).

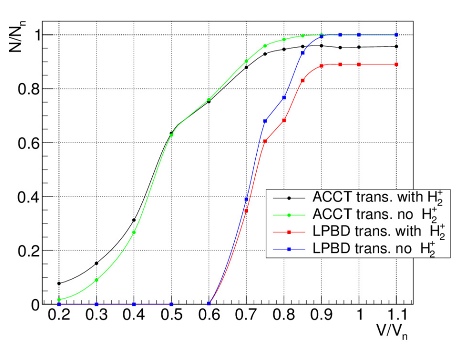

Figure 7: Transmission curve for 13 mA extracted current proton beam with 61.5% proton fraction, in case the simulations take (or not) into account the H^+_2

This effect is very important because it can bias the measurement of the voltage calibration curve of the RFQ: as a matter of fact, the experimental transmission is given by I_{LPBD}/I_{LEBT}. Therefore, it depends on the value of I_{LEBT}, which generally also measure the residual component of contaminants that reaches the injection cone. Figure 7 shows a simulation on voltage calibration curve performed considering a low perveance beam (13 mA extracted proton beam current with 61.5% proton fraction). It is possible to see that the curve depends on including or not the contaminants contribute to I_{LEBT}. This may cause a down estimation of the current, which can be significant (> 10%).

PROTON RESULTS

The proton results presented here considers the low and half beam perveance. During the probe beam commissioning (low perveance), thanks to the presence of a permanent magnet we could measure the effect of contaminants onto the transmission, foresee by the simulations. Fig. 8 shows the combined effect of the steerers and the permanent magnet onto the transmission and current at the LPBD.

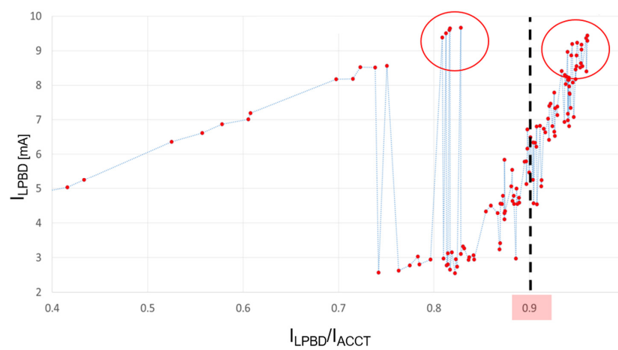

Figure 8: the plot shows some record of the current vs transmission in the RFQ for a low perveance beam of 10 mA proton beam, during the operation of an automatic steerer scan routine. The two regions of maximum currents are encircled. The 90% transmission level is shown.

Two regions are shown (with red circles) which present similar currents at the LPBD but corresponding to a not negligible different transmissions (82% and 98%). This was due to the contaminants, that were able, in one case, to be lost before the current monitor position in LEBT. After the first set of measurement of the probe beam, we increase the current up to roughly half perveance.

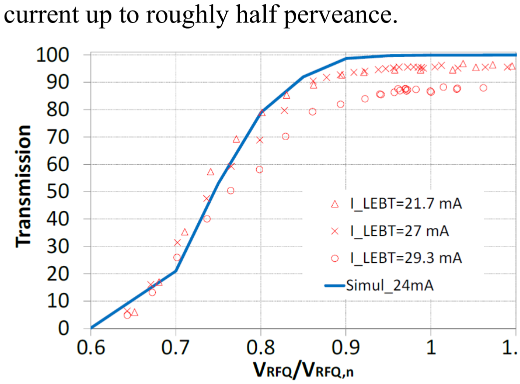

Figure 9: voltage calibration curve with several current points and simulated curve at 24 mA.

Figure 9 shows the voltage calibration curve with different currents at the LEBT ACCT. For comparison a simulation with 24 mA is also reported. It is worth to notice the

ISBN: 978-3-95450-225-7 ISSN: 2673-5571 doi:10.18429/JACoW-HB2021-WEDC2

measurement referring to 29.3 mA: its lower transmission, below 90%, was explained by the fact that its emittance was not compliant with $\varepsilon_{rms,t,n} < 0.2$ mm mrad criterion. Another important measurement was the transverse emittance after the RFQ [19]. We took some systematic data varying the LEBT solenoids and the voltage of the RFQ. We obtained satisfying benchmarking results, for the half proton beam, as shown in Fig. 10.

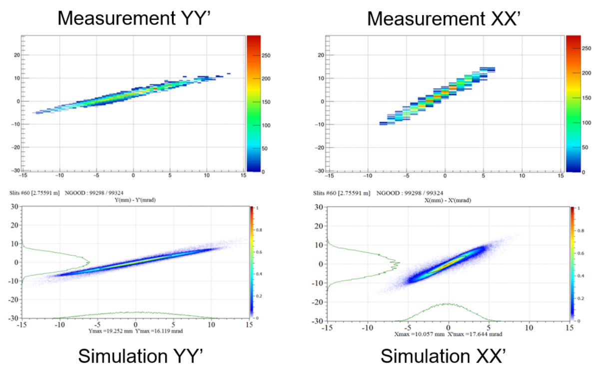

Figure 10: voltage calibration curve with several current points and simulated curve at 24 mA.

The larger simulated/measured relative differences on the rms emittances for the scan up to know performed is 16%. We obtained 13% on the betatrone's and 10% on the α.

DEUTERON RESULTS

This chapter presents the results of the RFQ beam dynamics performances at nominal perveance (125 mA accelerated beam, 0.1% D.C., 1 ms beam pulse [20]). Unlucky, the chopper was not functioning during this measurement shifts, and therefore we could not measure the transverse emittance at the exit of the RFQ and the profiles.

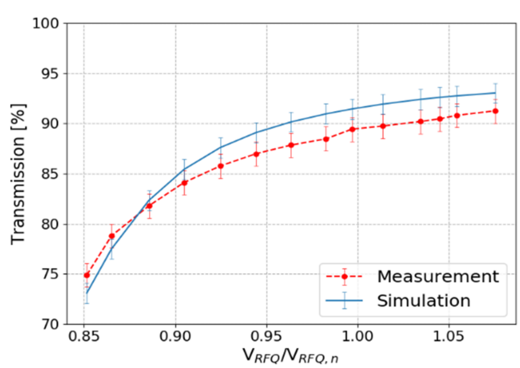

Figure 11: Voltage calibration curve of 136 mA deuteron beam. The simulation considers the effect of the contaminants. The data refer to the accelerated particle only.

These measurements will be performed in the future campaign. Fig. 11 shows the measurements and the simulation of the voltage calibration curve performed with 125 mA deuteron beam accelerated through the RFQ. During the same shift we measured the energy of the accelerated particles with the BMPs positioned after the RFQ (see Fig. 12). The results were in agreement with the neutron production on the LPBD and on the MEBT scrapers due to the reaction ^{27}Al(d,n) [21]

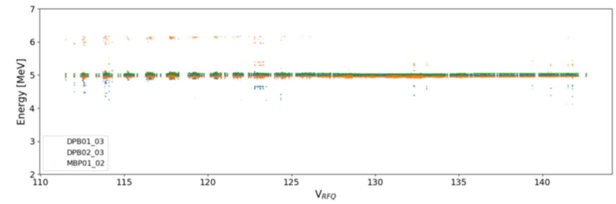

Figure 12: Energy measurement with respect the RFQ voltage.

Another interesting measurement performed with the BPMs [22] allowed us to measure the oscillations of the beam barycentre energy after the RFQ with respect the RFQ voltage. It turned out that we can connect such oscillations of the barycentre to the voltage offset of ± 1 kV of the 100 kV platform (see Fig. 13). A dedicated experiment is foreseen in the next campaign

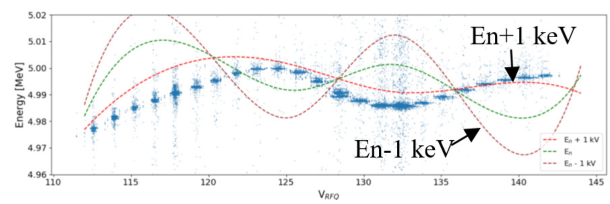

Figure 13: Energy measurement with respect the RFQ voltage. Simulation curves with different beam input energy (corresponding to V_{ext}/e) are shown.

CONCLUSIONS

The RFQ beam dynamics have been tested for two main regimes: the half and nominal perveance beams. The emittance at half perveance and the transmissions on both nominal and low current beams of the accelerated particles resulted compatible to the simulations. Table 3 summarizes the results for nominal beam perveance.

Table 3: Summary of the results on the 125 mA accelerated deuteron beam @ V/V$_n$=1. The emittances are in mm mrad.

Beam dist.	$\varepsilon_{rms,t,n}$	$\varepsilon_{99\%,t,n}$	Transm.
Experimental	/	/	89.7±1.2
Sim. D^+ and D_2^+	/	/	91.5±1.0
Sim. D^+	0.2	3.7	92.5±1.0
4D Gauss.	0.25	2.2	91.8 (as-b.), 93.7(design)

ACKNOWLEDGEMENTS

The present work was performed in the framework of the Broader Approach Agreement. The authors gratefully acknowledge the support of their home institutions and research funders for this work. Views and opinions expressed herein do not necessarily reflect those of QST, Fusion for Energy, or of the authors' home institutions or research funders.

ISBN: 978-3-95450-225-7 ISSN: 2673-5571 doi:10.18429/JACoW-HB2021-WEDC2

REFERENCES

[1] P. Cara *et al.*, "IFMIF/EVEDA Project: Achievements and Outlooks beyond 2020", presented at FEC'20, 650, unpublished.

[2] R. Gobin *et al.*, "Final Design of the IFMIF Injector at CEA/Saclay", in *Proc. IPAC'13,* Shanghai, China, May 2013, paper THPWO003, pp. 3758-3760.

[3] A. Pisent *et al.*, "IFMIF-EVEDA RFQ Design", in *Proc. EPAC'08,* Genoa, Italy, June 2008, paper THPP078, pp. 3542-3544.

[4] I. Podadera *et al*, "The Medium Energy Beam Transport Line (MEBT) of IFMIF/EVEDA LIPAc", in *Proc. IPAC'11*, San Sebastian, Spain, Sep. 2011, paper WEPS058, pp. 2628-2630.

[5] J. Marroncle *et al*, "IFMIF-LIPAc Diagnostics and its Challenges", in *Proc. IBIC'12*, Tsukuba, Japan, Oct. 2012, paper WECC01, pp. 557-565.

[6] E. Fagotti *et al.*, "Beam Commissioning of the IFMIF/EVEDA very high power RFQ", in *Proc. IPAC'18,* Vancouver, Canada, May 2018, pp. 2902-2907. doi:10.18429/JACoW-IPAC18-THXGBF2

[7] M. Comunian and A. Pisent, "Beam Dynamics Redesign of IFMIF-EVEDA RFQ for a Larger Input Beam Acceptance", in *Proc. IPAC'11*, San Sebastian, Spain, Sep. 2011, paper MOPS031, pp. 670-672.

[8] R. Douperrier, "TOUTATIS: A radio frequency quadrupole code", *Phys. Rev. Accel. Beams,* vol 3, p.124201, Dec. 2000. doi:10.1103/PhysRevSTAB.3.124201

[9] A. Palmieri *et al*, "Tuning the IFMIF 5MeV RFQ Accelerator", in *Proc. LINAC'16*, East Lansing, MI, USA, Sep. 2016, pp. 969-971. doi:10.18429/JACoW-LINAC2016-THPLR049

[10] T. P. Wangler, "RF Linear Accelerators", in *Physics Textbook,* John Wiley & Sons, Ltd, 2008 doi:10.1002/9783527623426

[11] L. Bellan *et al.*, "Extraction and low energy beam transport models used for the IFMIF/EVEDA RFQ commissioning", presented in ICIS'21, 25, unpublished.

[12] N. Chauvin *et al.*, "Deuteron beam commissioning of the linear IFMIF prototype accelerator ion source and low energy beam transport", *Nucl. Fusion,* vol. 59, p.106001, August 2019. doi:10.1088/1741-4326/ab1c88

[13] T. Akagi *et al.*, "Commissioning of high current H^+/D^+ ion beams for the prototype accelerator of the International Fusion Materials Irradiation Facility", *Rev. Sci. Instrum.,* vol. 91, p.023321, February 2020. doi:10.1063/1.5129598

[14] B. Bolzon *et al.*, "Intermediate Commissioning Results of the 70 mA/50 keV H+ and 140 mA/100 keV D+ ECR Injector of IFMIF/LIPAC", in *Proc. IPAC'16*, Busan, Korea, May 2016, pp. 2625-2627. doi:10.18429/JACoW-IPAC2016-WEPMY033

[15] L. Bellan *et al.*, "Source and LEBT Beam Preparation for IFMIF-EVEDA RFQ", in *Proc. LINAC'16*, East Lansing, MI, USA, Sep. 2016, pp. 420-423. doi:10.18429/JACoW-LINAC2016-TUPRC005

[16] T. Kalvas *et al., "*IBSIMU: A three-dimensional simulation software for charged particle optics", *Rev. Sci. Instrum.,* vol 81, p. 02B703, February 2010. doi:10.1063/1.3258608

[17] D.P. Grote and A. Freidman, "The WARP Code: Modeling High Intensity Ion Beams", *AIP Conf. Proc.,* vol. 749, p.55-58, March 2016. doi:10.1063/1.1893366

[18] http://irfu.cea.fr/en/Phocea/Page/index.php?id=780

[19] J. Marroncle *et al.*, "Transverse emittance in 2.5 MeV proton beam on LIPAc, IFMIF's Prototype", in *Proc. IBIC'19,* Malmö, Sweden, September 2019, pp. 288-293. doi:10.18429/JACoW-IBIC2019-TUPP006

[20] F. Grespan *et al*, "IFMIF/EVEDA RFQ Beam Commissioning at Nominal 125 mA Deuteron Beam in Pulsed Mode", presented at the IPAC'20, Caen, France, May 2020, paper TUVIR11. doi:10.18429/JACoW-IPAC2020-TUVIR11

[21] K. Kondo *et al.*, "Neutron production measurement in the 125-mA 5-MeV deuteron beam commissioning of Linear IFMIF Prototype Accelerator (LIPAc) RFQ", *Nucl. Fusion.* September 2021, accepted mauscript. doi: 10.1088/1741-4326/ac233c

[22] I. Podadera *et al.*, "Beam commissioning of beam position and phase monitors for LIPAc", in *Proc. IBIC'19,* Malmö, Sweden, September 2019, pp. 534-538. doi:10.18429/JACoW-IBIC2019-WEPP013